Technique of fetal echocardiography

Mi-Young Lee, Hye-Sung Won

Department of Obstetrics and Gynecology, University of Ulsan College of Medicine, Asan Medical Center, Seoul, Korea

Congenital heart disease is the most common abnormality in the human fetus. Fetal echocardiography has been used to detect the majority of cardiac defects, and it is now part of the routine screening method for fetal evaluation. In this article, we present standard ultrasonographic views of the normal fetal heart obtained during the second trimester, first-trimester fetal echocardiography findings, and a modified myocardial performance index.

Keywords: Congenital; Echocardiography; Fetal heart; Heart defects; Prenatal diagnosis

Introduction

Fetal echocardiography is an essential tool for screening of the fetal cardiac anatomy. Congenital heart disease is the most common abnormality in the human fetus, occurring in approximately 8–9 per 1,000 live births [1]. Prenatal diagnosis of cardiac defects is important because it allows families to receive appropriate counseling and to properly prepare for the birth of a child with congenital heart disease. Upon diagnosis of a cardiac defect, fetuses should be referred to a tertiary center for proper management. Two-dimensional imaging is still the gold standard and commonly used in fetal echocardiography. Therefore, we present standard views of the normal fetal heart obtained during the second trimester by two-dimensional ultrasound, and color and pulsed wave Doppler. We also present first-trimester fetal echocardiographic findings and a modified myocardial performance index (Mod-MPI), which is a useful tool for evaluating fetal cardiac function.

Determining the abdominal situs

Before scanning the fetal heart, it is important to determine whether abdominal situs is normal because congenital heart diseases are frequently associated with abnormal abdominal situs. On the basis of fetal position, several planes can exist. In a fetus with breech presentation, the left side of the fetus should be proximal to the transducer when the fetal occiput is on the left side of the mother (Fig. 1A). When the fetal occiput is on right side of the mother, the left side of the fetus should be distal to the transducer (Fig. 1B). When the fetus is positioned face up, its left side appears on the right side of the screen, and when the fetus is lying face down, its left side appears on the same side of the screen. In a fetus with vertex presentation, determination of abdominal situs is reversed (Fig. 1C, D). While it can be difficult to determine abdominal situs when the fetus is in the transverse position, the right–hand rule of thumb can reliably determine fetal situs (Fig. 2) [2]. With this simple approach, the palm of the right hand corresponds to the fetal abdomen, the dorsal side of the forearm to the fetal back, and the fist to the fetal head. The direction of the thumb always corresponds to the left side of the fetus regardless of the fetal position.
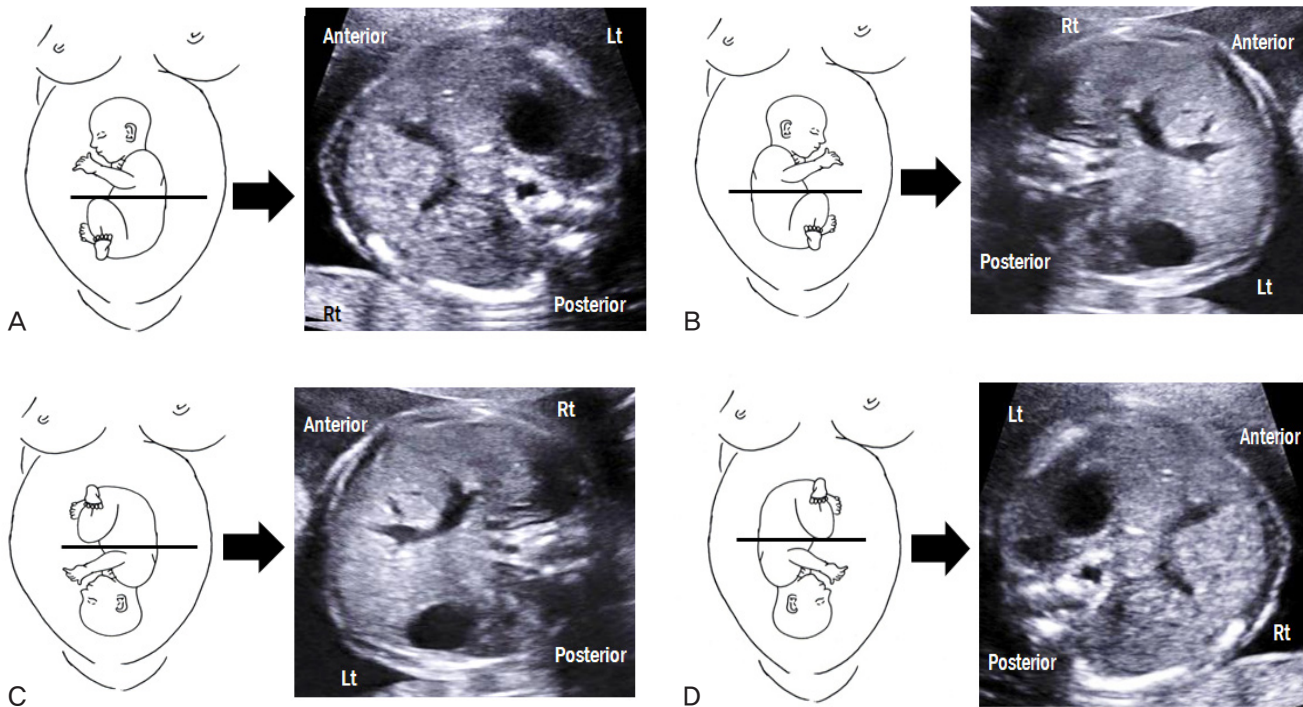
Fig. 1. Schematic images and transverse abdominal views of fetuses with breech and vertex presentations. (A) Breech presentation with fetal occiput on the maternal left side. (B) Breech presentation with fetal occiput on the maternal right side. (C) Vertex presentation with fetal occiput on the maternal left side. (D) Vertex presentation with fetal occiput on the maternal right side.
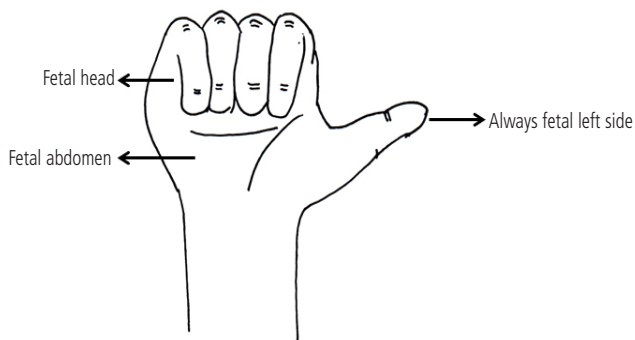

Fig. 2. Right-hand rule of thumb for transabdominal scanning. The palm of the right hand corresponds to the fetal abdomen, the dorsal side of the forearm to the fetal back, and the fist to the fetal head. The direction of the thumb always corresponds to the left side of the fetus.

Transverse view of the abdomen

A transverse abdominal view is shown in Fig. 3. The stomach and liver are located on the left and right, respectively. The descending aorta (DAo) lies anterior and to the left of the spine, whereas the inferior vena cava (IVC) lies anterior and to the right of the DAo. By moving the transducer cranially, the car-
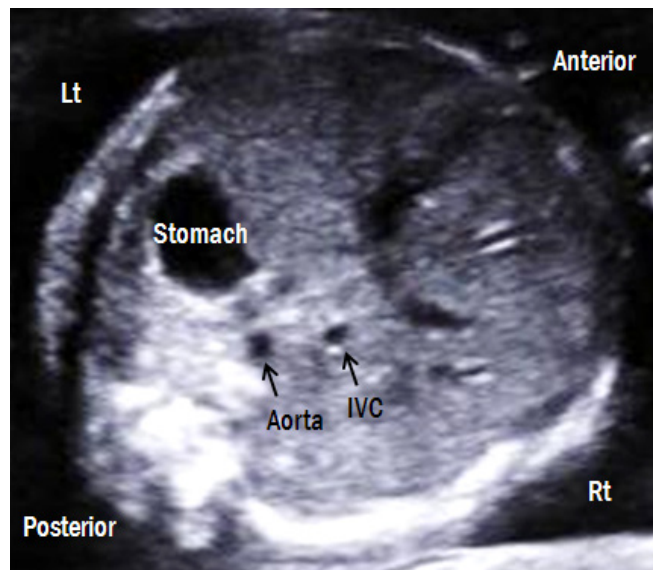

Fig. 3. Transverse abdominal view. The fetal stomach is on the left side and liver is on the right side. The descending aorta is posterior-left located and the IVC is anterior-right located. Lt, left; Rt, right; IVC, inferior vena cava.

diac apex should be located on the same side as the stomach. Abdominal situs abnormalities, such as those present in het-
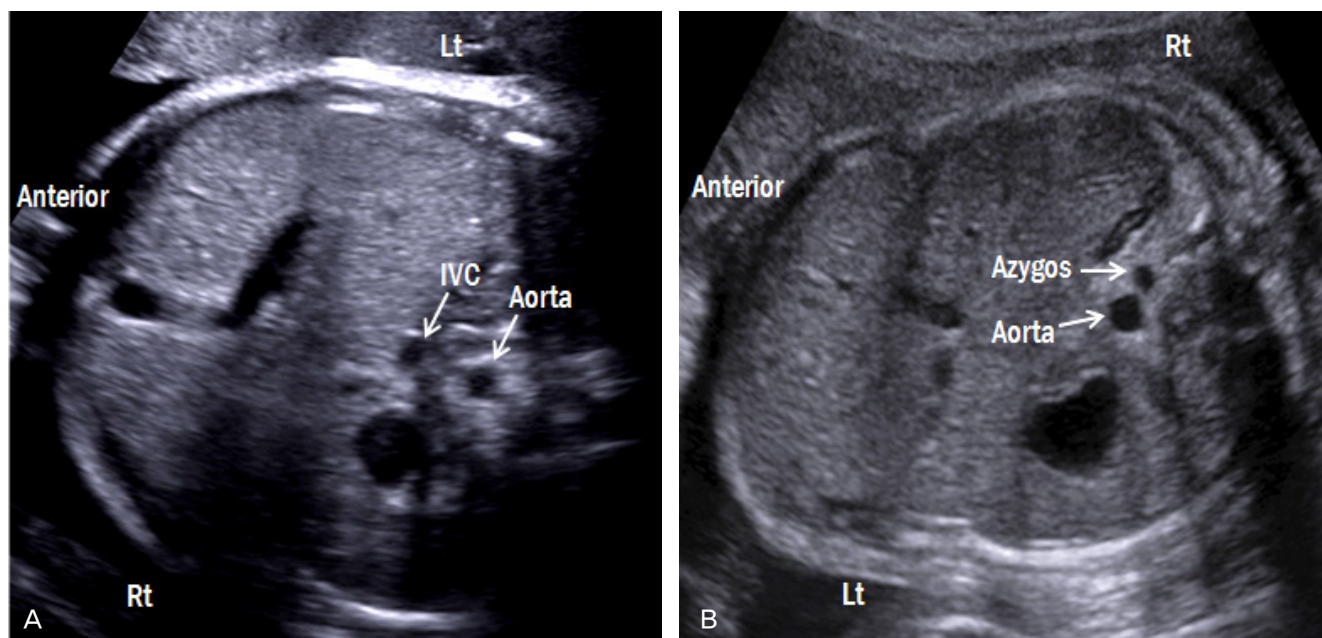
Fig. 4. Transverse abdominal views of both forms of heterotaxy syndrome. (A) Fetus with right atrial isomerism (breech presentation) shows juxtaposition of the aorta and IVC on either left side of the spine. The right-sided stomach and the midline liver are also shown. (B) Fetus with left atrial isomerism (vertex presentation) shows invisible IVC with dilated azygos vein, suggestive of an interrupted IVC with azygos vein continuation. Lt, left; Rt, right; IVC, inferior vena cava.

erotaxy syndrome, can be detected with careful observation of this view (Fig. 4).

Four-chamber view

The four-chamber view (4CV) is not only the easiest view to obtain, but also the most important view of the fetal heart. The 4CV is easily visible by moving the transducer cranially from the transverse abdominal view (Fig. 5A). Approximately 60% of congenital heart disease cases are detected with this view [3]. Examiners should carefully assess heart structure to rule out congenital heart disease, using the following criteria:

1) A normal heart is approximately one-third of the thorax in size, and this proportion (cardiothoracic area, C/T area) is constant throughout gestation [4]. When the C/T area is greater than two standard deviations, cardiomegaly may be suspected [5].
2) The cardiac axis lies at a 45° angle to the left of the midline [6].
3) The two atria are equal in size and separated by the atrial septum. The flap of foramen ovale lies in the left atrial cavity.

4) The two atrioventricular valves are equally opened and differentially inserted: the septal leaflet of the tricuspid valve is inserted more apically than the mitral valve in the ventricular septum. Blood flow across both valves should be evaluated by color Doppler imaging to ensure that both ventricles fill equally in diastole without regurgitation (Fig. 5B). Doppler waveforms across both atrioventricular valves are shown in Fig. 5C, D. The E wave, which corresponds to the early ventricular filing of diastole, is followed by the A wave, which corresponds to the active ventricular filling of diastole (atrial contraction). The A wave is always higher than E wave in the normal fetus. The peak velocity of both waves is 30–60 cm/sec, and is constant throughout gestation [7].
5) The crux of the heart, the area of junction of atrial septum, atrioventricular valves, and interventricular septum are intact.
6) The two ventricles are equal in size, although the right side of the heart becomes larger as gestation progresses [8].
7) The right ventricle contains the moderator band.
8) The ventricular septum is intact.
9) Pulmonary veins are connected to the left atrium.
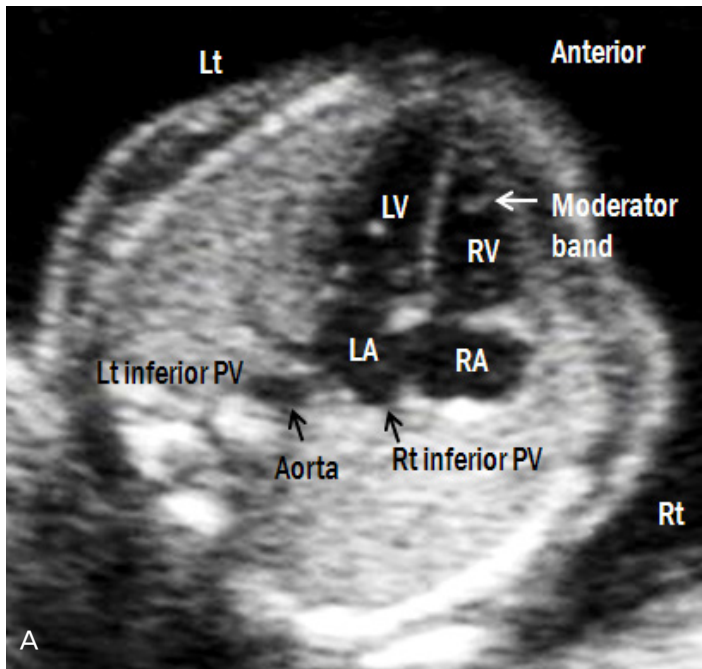10) The DAo is located anterior and to the left of the spine.

Fig. 5. (A) Apical four-chamber view of the fetal heart. (B) Color Doppler image shows forward flow from both atria to both ventricles. (C) Doppler waveforms of tricuspid and (D) mitral valves show a biphasic pattern. The E wave corresponds to early ventricular filing of the diastole, and the A wave corresponds to active ventricular filling of the diastole (atrial contraction). (D) Because of the continuity between mitral and aortic valves, the Doppler waveform at the mitral valve shows aortic outflow. Lt, left; Rt, right; LA, left atrium; RA, right atrium; LV, left ventricle; RV, right ventricle; PV, pulmonary vein.
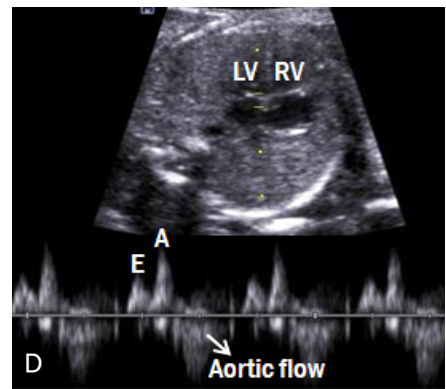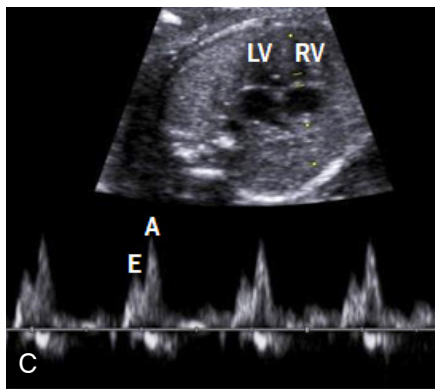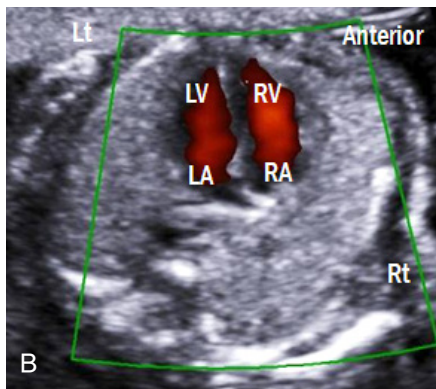
Beside the evaluation of 4CV, assessment of great arteries' connections further detects about 90% of serious congenital heart diseases [3].

Left ventricular outflow tract view

A slight tilt of the transducer from the lateral 4CV, which is positioned the ventricular septum perpendicular to the ultrasound beam, toward the cardiac apex yields a left ventricular outflow tract (Fig. 6A). This view shows the left ventriculoarterial connection as well as the intact ventricular septum. Blood flow across the aortic valve is laminar flow with no turbulence in systole and no regurgitation in diastole (Fig. 6B). Peak systolic velocity in the aorta increases linearly with advancing gestation, and it ranges from approximately 30 cm/sec at 19

weeks to 100 cm/sec at full term [9,10]. Peak systolic velocity in the aorta is greater than in the pulmonary artery [11].

Right ventricular outflow tract view

This view is obtained by sweeping the transducer from left ventricular outflow tract to the fetal head (Fig. 7A). The crossing nature of the great arteries can be confirmed by moving the transducer slightly up and down. This view demonstrates the right ventriculoarterial connection. Using color Doppler imaging, laminar flow across the pulmonary valve is confirmed (Fig. 7B). Peak systolic velocity in the pulmonary artery also increases linearly with advancing gestation, and it reaches 100 cm/sec at full term [10,11].
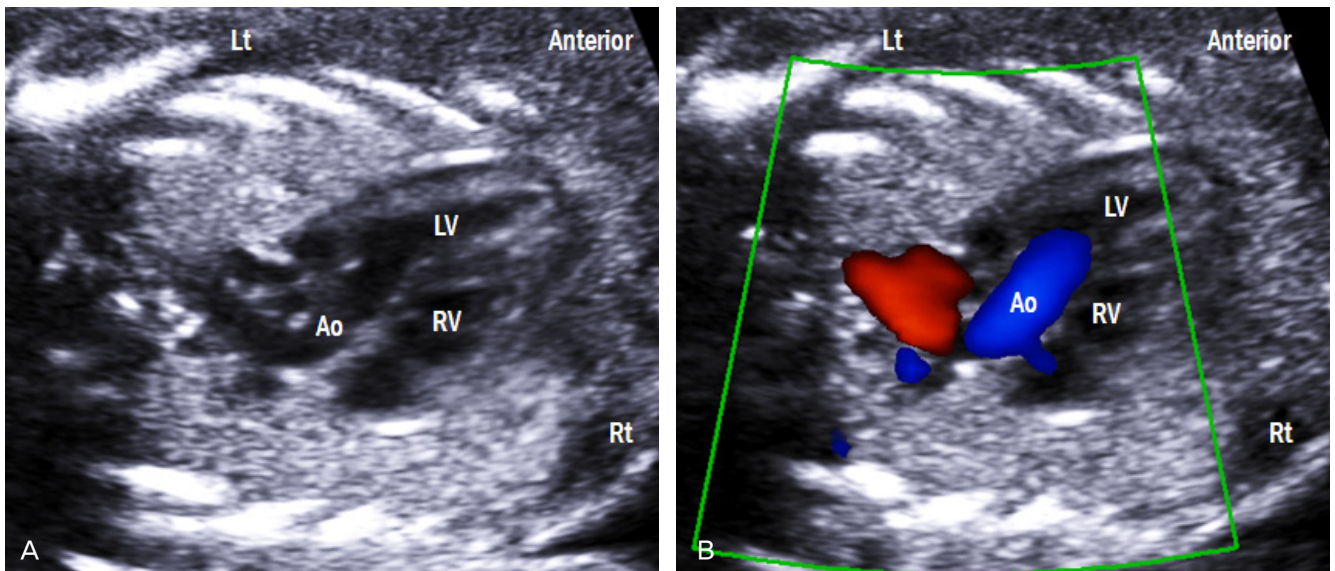
Fig. 6. Left ventricular outflow tract view. (A) This view shows the ventriculoarterial connection and intact ventricular septum. (B) Color Doppler across the aortic valve shows laminar flow and no turbulence in systole. Lt, left; Rt, right; LV, left ventricle; RV, right ventricle; Ao, aorta.
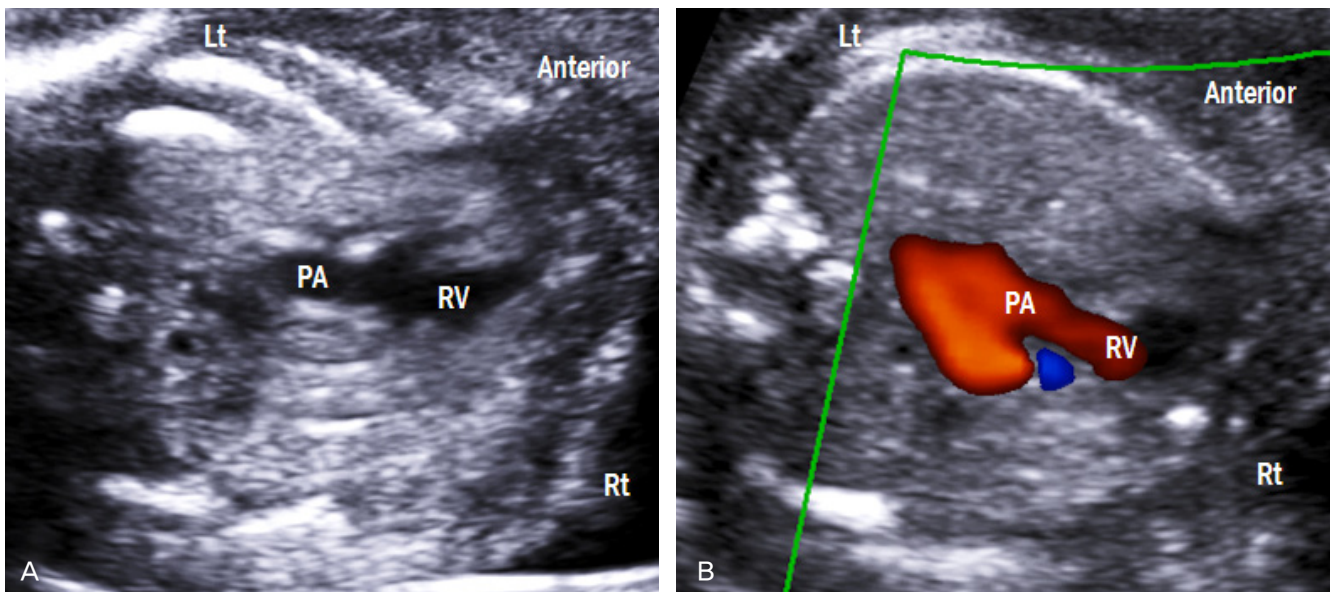

Fig. 7. Right ventricular outflow tract view. (A) This view shows the right ventriculoarterial connection. (B) Color Doppler image demonstrates laminar flow across the pulmonary valve. Lt, left; Rt, right; RV, right ventricle; PA, pulmonary artery.

Three-vessel view

This view is obtained by moving the transducer cranially maintaining a transverse position from the 4CV (Fig. 8). The main pulmonary artery, ascending aorta, and superior vena cava (SVC) are arranged in a straight line from the left anterior to the right posterior aspect. The pulmonary artery is the largest in size, followed by the ascending aorta and the superior vena cava. The main pulmonary artery is divided into left and right pulmonary arteries. The thymus is also clearly visible in this view. The three-vessel view (3VV) is useful in diagnosing conotruncal cardiac abnormalities [12].
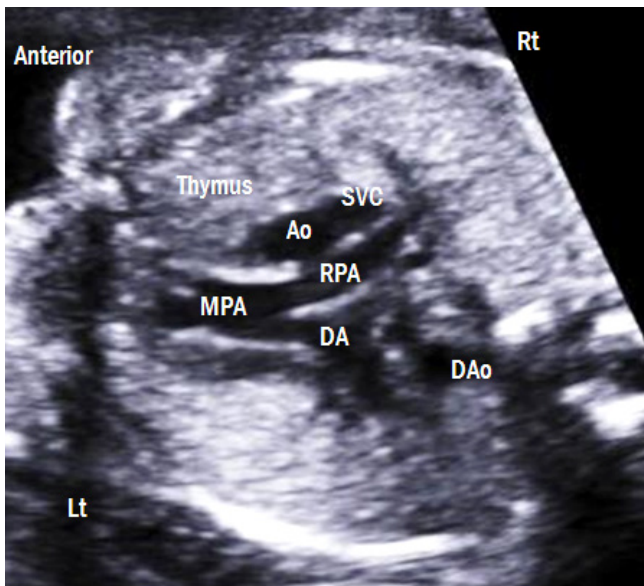
Fig. 8. Three-vessel view. The main pulmonary artery, ascending aorta, and superior vena cava are arranged in a straight line from the left anterior to the right posterior aspect. The pulmonary artery is the largest in size, followed by the ascending aorta and the superior vena cava. The thymus is clearly visible anterior to the three vessels. Lt, left; Rt, right; MPA, main pulmonary artery; RPA, right pulmonary artery; DA, ductus arteriosus; Ao, aorta; SVC, superior vena cava; DAo, descending aorta.

Three-vessel-trachea view (transverse aortic and ductal arch view)

Aortic and ductal arches are combined into the DAo, which appear as a V-shaped confluence (Fig. 9A). Both arches are similar in size and located to the left side of the trachea. The thymus is also visible in this view. Color Doppler imaging demonstrates the same direction of blood flow in both arches (Fig. 9B). This view allows comparison of both arches and assessment of aortic arch abnormalities, including aortic arch hypoplasia and coarctation of the aorta [13].

Aortic arch view

By rotating the transducer 90 degree either clockwise or counterclockwise from the 3VV, a 'candy cane-like' aortic arch is seen (Fig. 10A). The aortic arch gives rise to the three arterial branches, namely, the brachiocephalic, left common carotid, and left subclavian arteries. All three branches are clearly visible by color Doppler imaging (Fig. 10B). Because the innominate vein is the largest vessel in the mediastinum, it is often observed in front of the brachiocephalic artery [14].

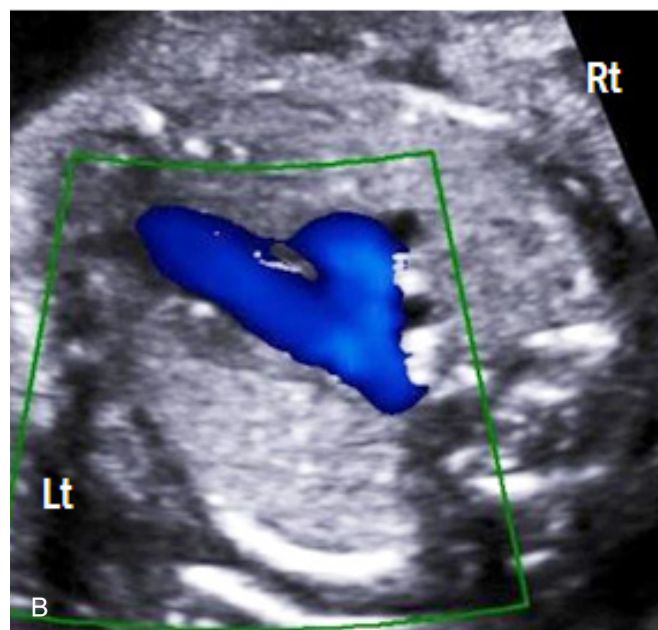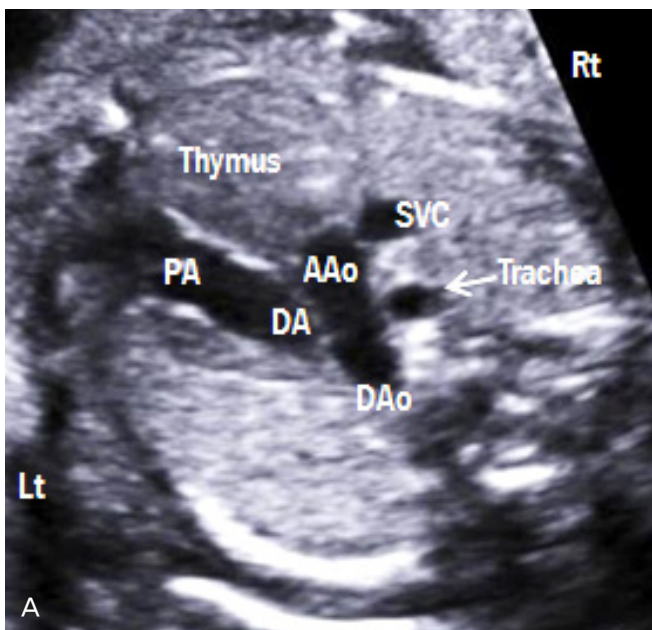**Fig. 9.** Three-vessel-trachea view. (A) This view demonstrates a V-shaped confluence of aortic and ductal arches at the descending aorta. (B) The trachea is located to the right side of the aorta. Color Doppler shows the same direction of blood flow in both arches. Lt, left; Rt, right; PA, pulmonary artery; DA, ductus arteriosus; AAo, ascending aorta; DAo, descending aorta; SVC, superior vena cava.
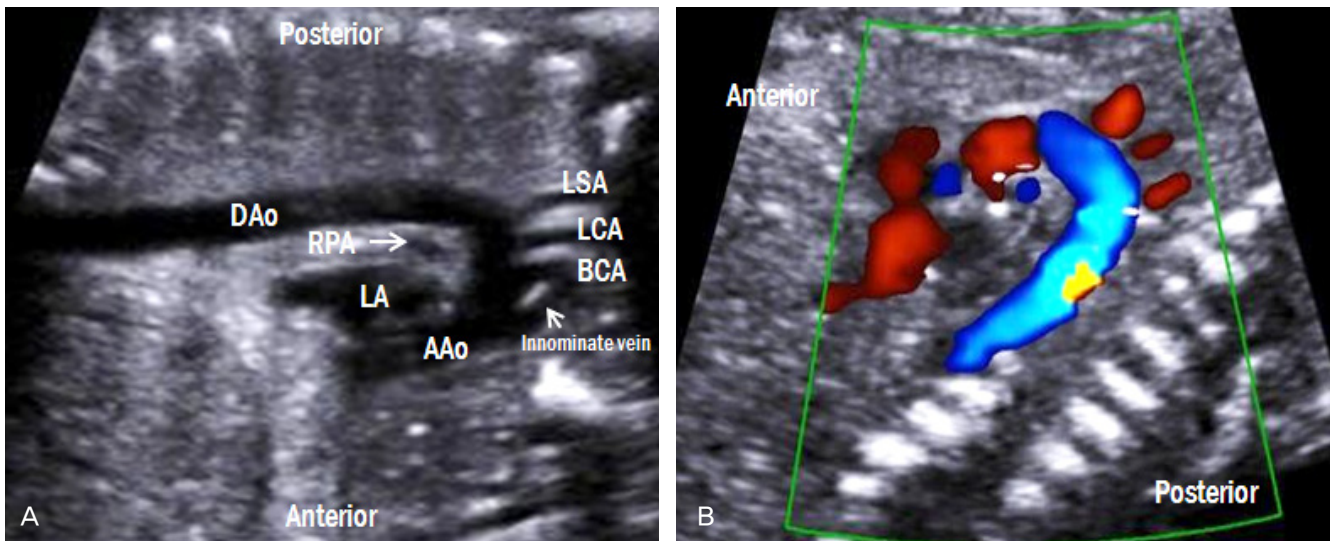
Fig. 10. Aortic arch view. (A) A 'candy cane-like' aorta gives rise to the three arterial branches, namely, the brachiocephalic, left common carotid, and left subclavian arteries. (B) These three branches are also visible by color Doppler imaging. LA, left atrium; RPA, right pulmonary artery; AAo, ascending aorta; DAo, descending aorta; BCA, brachiocephalic artery; LCA, left common carotid artery; LSA, left subclavian artery.
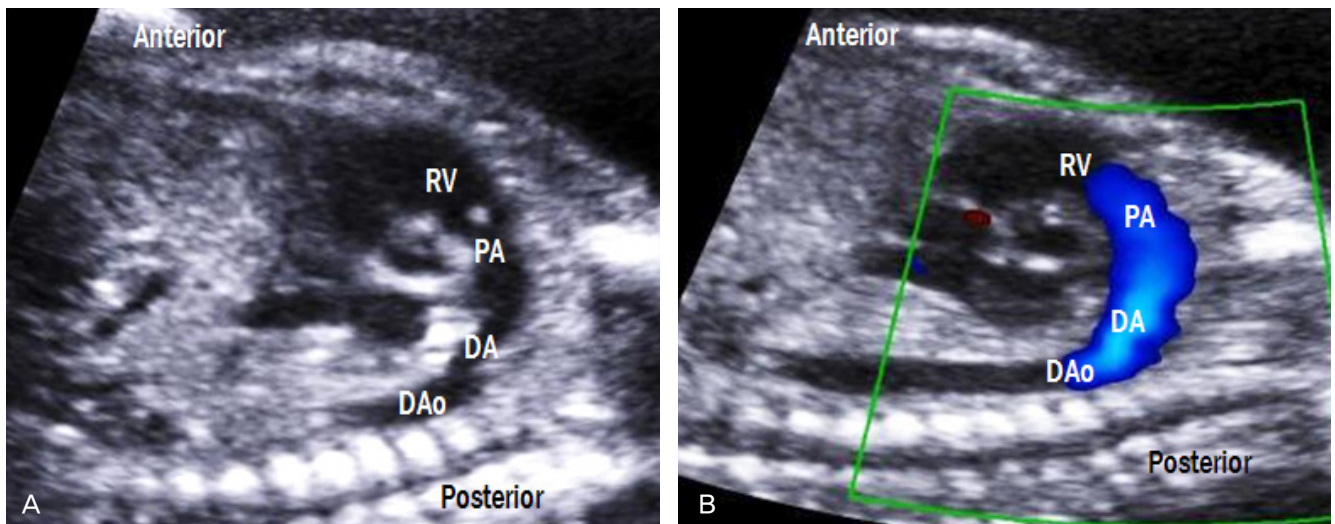

Fig. 11. Ductal arch view. (A) The ductus arteriosus connects the main pulmonary artery to the DAo, forming hockey stick-shaped arch. (B) Laminar flow across the pulmonary valve is also shown. RV, right ventricle; PA, pulmonary artery; DA, ductus arteriosus; DAo, descending aorta.

Ductal arch view

By sliding the transducer from the aortic arch view to the left, a 'hockey stick-like' ductal arch is visualized (Fig. 11). This view mainly shows the right ventricle, pulmonary valve, and main pulmonary artery, which is connected to the DAo through the ductus arteriosus. Unlike the aortic arch, the ductal arch does not give rise to any branches.

Bicaval view (SVC and IVC view)

This view is obtained in a right parasagittal plane (Fig. 12). The SVC and IVC drain into the posterior aspect of the right atrium. The SVC and IVC are similar in size; however, the IVC is widened as it enters the right atrium because of interflow from the ductus venosus and hepatic veins.

First-trimester screening of fetal heart

Advancements in ultrasonography have paved the way for first-trimester fetal echocardiography since the 1990s [15-17]. Fetal echocardiography performed during the first-trimester is advantageous for at least two reasons. First, early diagnosis of cardiac defects allows families to make well-thought-out plans (i.e., to receive counseling, and/or prepare for the birth of a child with a congenital heart disease). Second, early screening relieves the anxiety of high risk patients who have previous family history of cardiac defects.

The examination of the fetal heart during early gestation includes the normal situs, cardiac axis, cardiac connections, atrioventricular junction, and septoaortic continuity [18]. If these structures are normal, most structural abnormalities can be excluded. The ultrasonographic findings of a normal heart at 13 weeks of gestation are shown in Fig. 13. Furthermore, increased nuchal translucency and abnormal ductus venosus flow increase the risk of not only chromosomal anomalies, but also congenital heart disease [19,20]. Therefore, these indicators are important for early detection of cardiac defects.
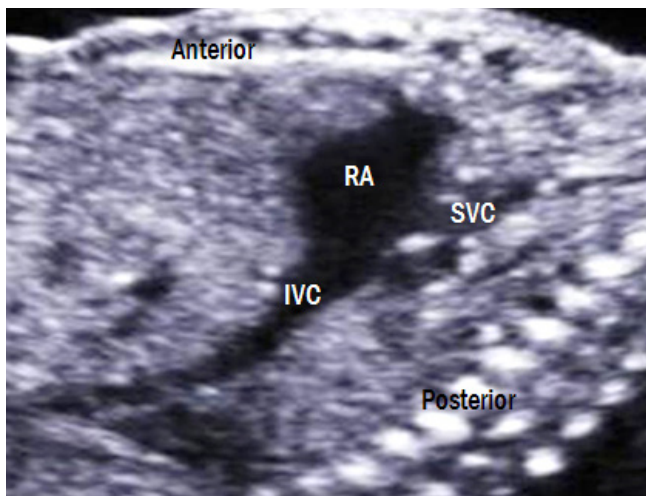

Fig. 12. Bicaval view. The SVC and IVC drain into the posterior aspect of the right atrium. The IVC is widened as it enters the right atrium because of interflow from the ductus venosus and hepatic veins. RA, right atrium; IVC, inferior vena cava; SVC, superior vena cava.

Modified myocardial performance index

Assessment of fetal cardiac function is now considered as a routine evaluation of fetal status. MPI was originally proposed by Tei et al. [21] for the evaluation of cardiac function in adults. MPI is calculated as the sum of the isovolumetric contraction time and isovolumetric relaxation time divided by the ejection time. Hernandez-Andrade et al. [22] further modified MPI, and this method is now commonly used (Fig. 14). The Mod-MPI is useful tool for evaluating fetal cardiac function in several conditions, such as intrauterine growth retardation, pre-eclampsia, maternal diabetes, and twin-to-twin transfusion syndrome [23-26]. It is also useful in planning for fetal therapy or childbirth.
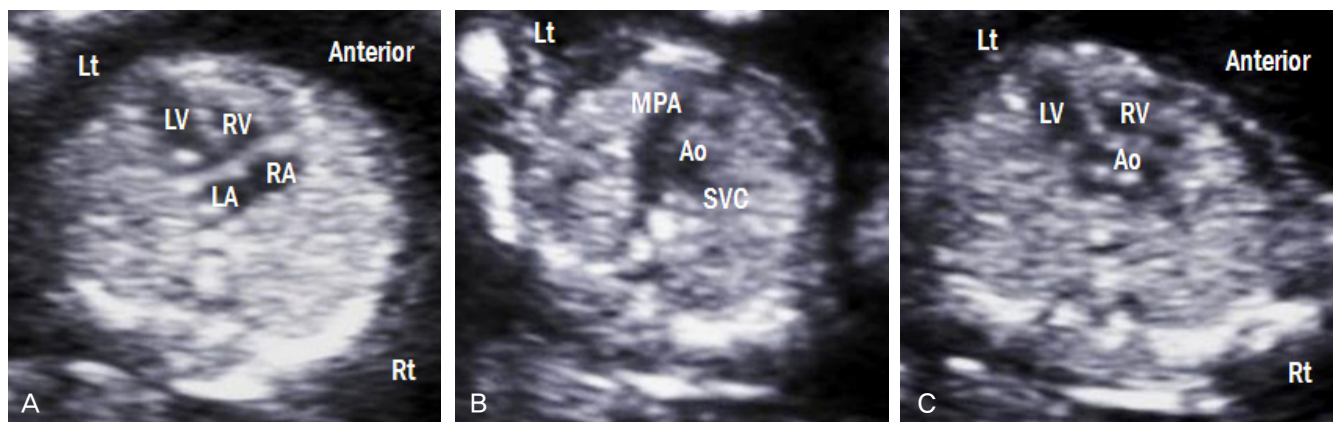

Fig. 13. Ultrasonographic images of fetuses with a normal heart at 13 weeks of gestation. (A) Four-chamber view. (B) Three-vessel view. (C) Left ventricular outflow tract view. Lt, left; Rt, right; LA, left atrium; RA, right atrium; LV, left ventricle; RV, right ventricle; MPA, main pulmonary artery; Ao, aorta; SVC, superior vena cava.
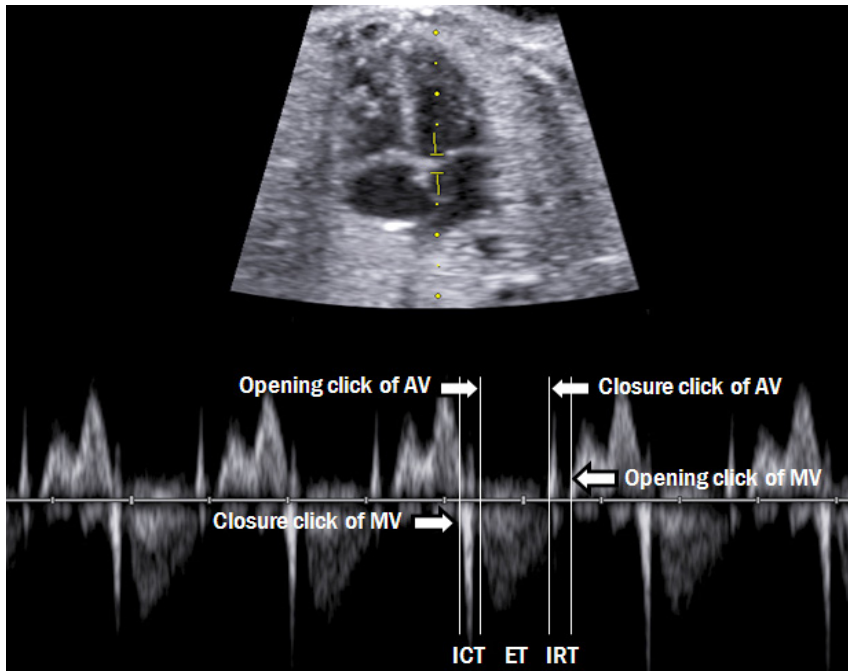
Fig. 14. Measurement of the fetal modified myocardial performance index. Each cursor should be placed at the beginning of each valve click, and the modified myocardial performance index is calculated as the sum of ICT and IRT divided by ejection time. AV, aortic valve; MV, mitral valve; ICT, isovolumetric contraction time; IRT, isovolumetric relaxation time; ET, ejection time.

Conclusion

Fetal echocardiography is a part of the routine evaluation of normal fetus. The prenatal diagnosis of cardiac defects depends on the knowledge, skill, and experience of practitioners. Therefore, obstetricians should be completely familiar with abovementioned anatomy of the fetal heart in order to detect any abnormalities that might be present.

Conflict of interest

No potential conflict of interest relevant to this article was reported.

References

1. Hoffman JI, Christianson R. Congenital heart disease in a cohort of 19,502 births with long-term follow-up. Am J Cardiol 1978;42:641-7.
2. Bronshtein M, Gover A, Zimmer EZ. Sonographic definition of the fetal situs. Obstet Gynecol 2002;99:1129-30.
3. Allan LD. A practical approach to fetal heart scanning. Semin Perinatol 2000;24:324-30.
4. Paladini D, Chita SK, Allan LD. Prenatal measurement of cardiothoracic ratio in evaluation of heart disease. Arch Dis Child 1990;65:20-3.
5. Chaoui R, Bollmann R, Goldner B, Heling KS, Tennstedt C. Fetal cardiomegaly: echocardiographic findings and outcome in 19 cases. Fetal Diagn Ther 1994;9:92-104.
6. Comstock CH. Normal fetal heart axis and position. Obstet Gynecol 1987;70:255-9.
7. Allan L. Technique of fetal echocardiography. Pediatr Cardiol 2004;25:223-33.
8. Jung E, Won HS, Lee PR, Kim A, Park IS. Clinical implication of isolated right dominant heart in the fetus. Prenat Diagn 2007;27:695-8.
9. Rizzo G, Arduini D, Romanini C. Doppler echocardiographic assessment of fetal cardiac function. Ultrasound Obstet Gynecol 1992;2:434-45.
10. Allan LD, Chita SK, Al-Ghazali W, Crawford DC, Tynan M. Doppler echocardiographic evaluation of the normal human fetal heart. Br Heart J 1987;57:528-33.
11. Reed KL, Anderson CF, Shenker L. Fetal pulmonary artery and aorta: two-dimensional Doppler echocardiography. Obstet Gynecol 1987;69:175-8.
12. Yoo SJ, Lee YH, Kim ES, Ryu HM, Kim MY, Choi HK, et al. Three-vessel view of the fetal upper mediastinum: an easy means of detecting abnormalities of the ventricular

outflow tracts and great arteries during obstetric screening. Ultrasound Obstet Gynecol 1997;9:173-82.

13. Pasquini L, Mellander M, Seale A, Matsui H, Roughton M, Ho SY, et al. Z-scores of the fetal aortic isthmus and duct: an aid to assessing arch hypoplasia. Ultrasound Obstet Gynecol 2007;29:628-33.

14. Abuhamad A, Chaoui R. The great vessels. In: Abuhamad A, Chaoui R, editors. A practical guide to fetal echocardiography. 2nd ed. Philadelphia (PA): Lippincott Williams & Wilkins; 2010. p.60-76.

15. Gembruch U, Knopfle G, Chatterjee M, Bald R, Hansmann M. First-trimester diagnosis of fetal congenital heart disease by transvaginal two-dimensional and Doppler echocardiography. Obstet Gynecol 1990;75:496-8.

16. Bronshtein M, Zimmer EZ, Milo S, Ho SY, Lorber A, Gerlis LM. Fetal cardiac abnormalities detected by transvaginal sonography at 12-16 weeks' gestation. Obstet Gynecol 1991;78:374-8.

17. Gembruch U, Knopfle G, Bald R, Hansmann M. Early diagnosis of fetal congenital heart disease by transvaginal echocardiography. Ultrasound Obstet Gynecol 1993;3:310-7.

18. Carvalho JS, Moscoso G, Tekay A, Campbell S, Thilaganathan B, Shinebourne EA. Clinical impact of first and early second trimester fetal echocardiography on high risk pregnancies. Heart 2004;90:921-6.

19. Hyett JA, Perdu M, Sharland GK, Snijders RS, Nicolaides KH. Increased nuchal translucency at 10-14 weeks of gestation as a marker for major cardiac defects. Ultrasound Obstet Gynecol 1997;10:242-6.

20. Matias A, Huggon I, Areias JC, Montenegro N, Nicolaides KH. Cardiac defects in chromosomally normal fetuses with abnormal ductus venosus blood flow at 10-14 weeks. Ultrasound Obstet Gynecol 1999;14:307-10.

21. Tei C, Ling LH, Hodge DO, Bailey KR, Oh JK, Rodeheffer RJ, et al. New index of combined systolic and diastolic myocardial performance: a simple and reproducible measure of cardiac function—a study in normals and dilated cardiomyopathy. J Cardiol 1995;26:357-66.

22. Hernandez-Andrade E, Lopez-Tenorio J, Figueroa-Diesel H, Sanin-Blair J, Carreras E, Cabero L, et al. A modified myocardial performance (Tei) index based on the use of valve clicks improves reproducibility of fetal left cardiac function assessment. Ultrasound Obstet Gynecol 2005;26:227-32.

23. Api O, Emeksiz MB, Api M, Ugurel V, Unal O. Modified myocardial performance index for evaluation of fetal cardiac function in pre-eclampsia. Ultrasound Obstet Gynecol 2009;33:51-7.

24. Hernandez-Andrade E, Crispi F, Benavides-Serralde JA, Plasencia W, Diesel HF, Eixarch E, et al. Contribution of the myocardial performance index and aortic isthmus blood flow index to predicting mortality in preterm growth-restricted fetuses. Ultrasound Obstet Gynecol 2009;34:430-6.

25. Figueroa H, Silva MC, Kottmann C, Viguera S, Valenzuela I, Hernandez-Andrade E, et al. Fetal evaluation of the modified-myocardial performance index in pregnancies complicated by diabetes. Prenat Diagn 2012;32:943-8.

26. Van Mieghem T, Klaritsch P, Done E, Gucciardo L, Lewi P, Verhaeghe J, et al. Assessment of fetal cardiac function before and after therapy for twin-to-twin transfusion syndrome. Am J Obstet Gynecol 2009;200:400.e1-7.